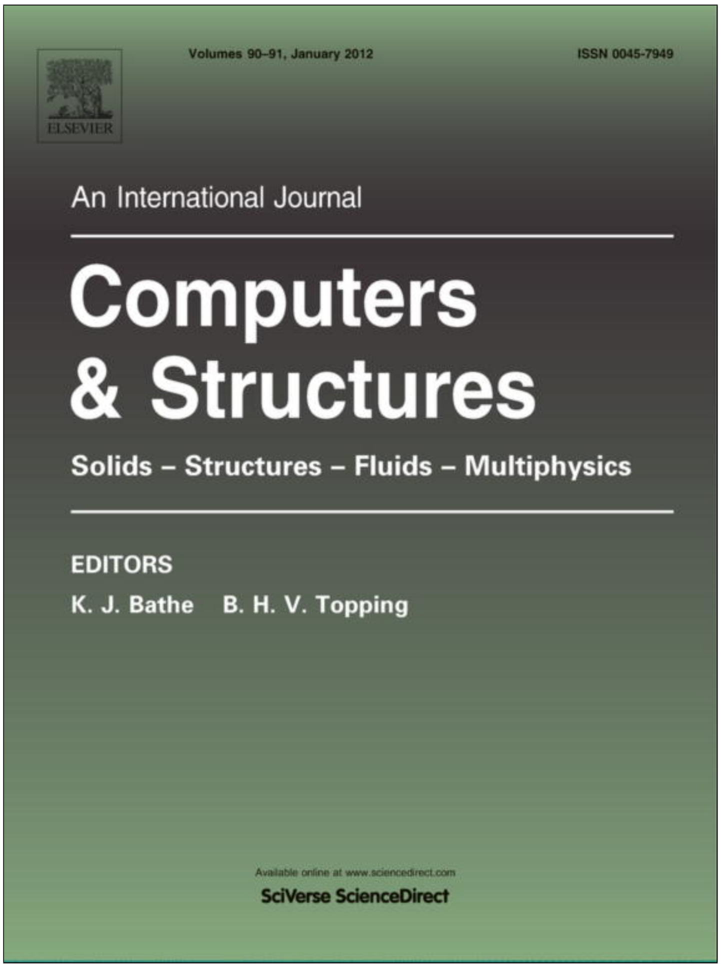
Volumes 90–91, January 2012
ISSN 0045-7949
ELSEVIER
An International Journal
Computers & Structures
Solids – Structures – Fluids – Multiphysics
EDITORS
K. J. Bathe B. H. V. Topping
Available online at www.sciencedirect.com
SciVerse ScienceDirect

Computers and Structures 90–91 (2012) 107–115

Contents lists available at SciVerse ScienceDirect

Computers and Structures

journal homepage: www.elsevier.com/locate/compstruc

# Radial basis functions-differential quadrature collocation and a unified formulation for bending, vibration and buckling analysis of laminated plates, according to Murakami's Zig-Zag theory

J.D. Rodrigues [a], C.M.C. Roque [a], A.J.M. Ferreira [b,*], M. Cinefra [c], E. Carrera [c]

[a] INEGI, Faculdade de Engenharia, Universidade do Porto, Rua Dr. Roberto Frias, 4200-465 Porto, Portugal
[b] Departamento de Engenharia Mecânica, Faculdade de Engenharia, Universidade do Porto, Rua Dr. Roberto Frias, 4200-465 Porto, Portugal
[c] Department of Aeronautics and Aerospace Engineering, Politecnico di Torino, Corso Duca degli Abruzzi, 24, 10129 Torino, Italy

A R T I C L E I N F O

*Article history:*
Received 23 March 2011
Accepted 4 October 2011
Available online 5 November 2011

*Keywords:*
Composites
Plates
Vibrations
Buckling
Meshless methods

A B S T R A C T

In this paper, we propose to use the Murakami's Zig-Zag theory for the static, vibration and buckling analysis of laminated plates, by a local radial basis function-based differential quadrature (LRBFDQ) method. The equations of motion and the boundary conditions are obtained by the Carrera's unified formulation, and further interpolated by the LRBFDQ method. The LRBFDQ method combines the excellent approximation of derivatives by differential quadrature (DQ) in a local mesh-free framework by radial basis functions (RBFs). The present mesh-free, local approximation method shows excellent accuracy in the static, free vibration, and buckling analysis of thick isotropic and laminated plates.


## 1. Introduction

To avoid the computational effort of mesh generation in finite element methods, mesh-free methods are an interesting option, because only the information at points is required, without loosing accuracy for problems with arbitrary domain shapes. The authors have used the global RBF collocation method for the analysis of several plates [1,2]. For practical problems, the global collocation provides strong ill-conditioning which turns the problem sensitive to the shape parameter of the radial basis functions. Other studies using meshfree RPIM for the buckling analysis of Mindlin and FSDT plate theories can be found in [38–40].

A local meshfree alternative was recently proposed by Shu et al. [3,4] (the local radial basis function-based differential quadrature (LRBFDQ) method) that can be applied to solve problems of complex geometry, using the concept of differential quadrature (DQ). The DQ method was first proposed by Bellman et al. [5] back in 1972. In this method, the derivative at a mesh point along a mesh line is approximated by a linear weighted sum of the functional values at all the mesh points along the mesh line. Therefore, DQ can be considered as a global method, with accurate numerical results by using just a few mesh points. So far, DQ method has been efficiently applied to solve just a few engineering problems [6–10].

On the other hand, the local LRBFDQ method has a local support. By using radial basis functions with a local collocation, the ill-conditioning observed in the global RBF collocation decreases significatively. This allows for a better convergence of the method.

Multilayered structures, such as sandwich or laminated plates and shells, show a piece-wise continuous displacement field in the thickness direction. This change in slope between two adjacent layers, that are considered to be perfectly bonded together, is known as the zig-zag (ZZ) effect, see Fig. 1. The different transverse (both shear and normal components) deformability of the layers is the source of the ZZ effect. Furthermore, these transverse strains are linked with transverse shear and normal stresses that, for equilibrium reasons, are continuous at the each layer interface. These equilibrium conditions are known as interlaminar continuity (IC) for transverse stresses.

There are many two-dimensional theories that take into account ZZ and IC in multilayered structures [11–16]. Some of these have been developed in the framework of layer-wise (LW) models, in which the number of the unknown variables depend on the number of layers, but they could result computational expensive, for laminates with large number of layers. Other theories have been formulated in the framework of equivalent single-layer (ESL) models, in which the unknown variables are the same for the whole laminate. Among these, Murakami [17] introduced a function of the thickness coordinate able to emulate the ZZ effect (MZZF). From implementation point of view, the inclusion of MZZF

* Corresponding author.
*E-mail address:* ferreira@fe.up.pt (A.J.M. Ferreira).

0045-7949/$ - see front matter © 2011 Elsevier Ltd. All rights reserved.
doi:10.1016/j.compstruc.2011.10.003

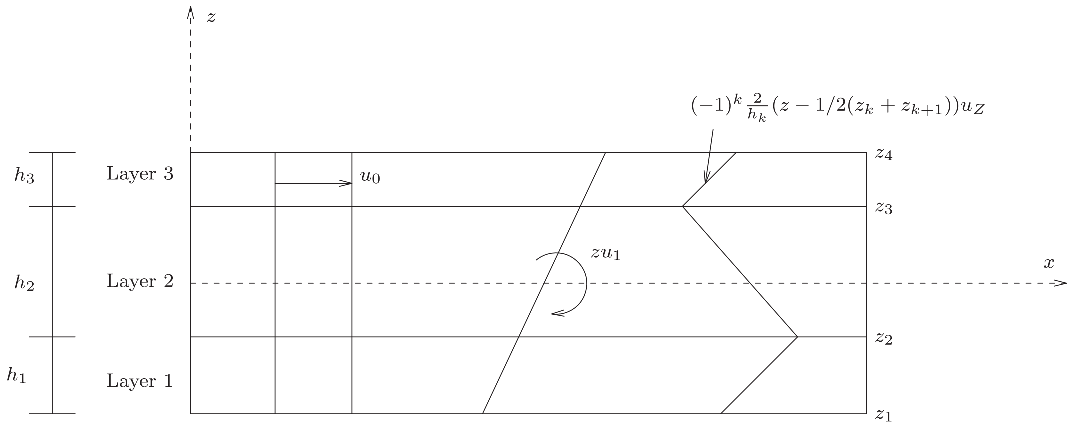


**Fig. 1.** Scheme of the zig-zag assumptions for a three-layered laminate.

in existing plate models requires the same efforts that are required by the inclusion of an additional degree of freedom. On the other hand, from numerical point of view, as it will be clear in this paper, inclusion of MZZF leads to significant improvements of the existing plate theories. An historical review on zig-zag theories has been provided by Carrera [16].

An extensive evaluation of the use of MZZF has been made in the framework of Carrera's unified formulation (CUF) [18]. The CUF is a powerful tool that permits to handle in a unified manner all the variables and fields of a considered problem, by calculating the so-called 'fundamental nuclei', that do not depend on the order of expansion in the thickness direction and the number of layers in the structure. Therefore, the MZZF can be easily introduced in the ESL models contained in the CUF and the efficiency of such extension has been largely proved in [19–21] using an analytical formulation and in [22] using the finite element method. In recent authors works, the CUF has been also combined with radial basis functions (RBF) and radial basis functions-finite difference (RBF-FD) methods to analyze laminated plates [23,24].

In the present work the attention is restricted to the application of ZZF to bending, vibration and buckling analysis of laminated plates, using the Murakami's ZZ displacement field [17], which allows for through-the-thickness deformations. The governing equations and the boundary conditions are obtained via the CUF in order to apply the LRBFDQ method for solving the static and dynamic problems. The quality of the present method in predicting static deformations, free vibrations and buckling loads of thin and thick laminated plates is compared and discussed with other methods in some numerical examples.

## 2. The RBF-DQ method

The DQ method is a numerical technique that approximates a partial derivative of a function at a center point by a weighted sum of the values of the function at the points belonging to the supporting domain of the center point. For example, if we are interested in the computation of $\partial f/\partial x$ at the point $\mathbf{x}_i$ and the supporting domain is $\{\mathbf{x}_{i,1},\ldots,\mathbf{x}_{i,m}\}$, then we can write

$$\left.\frac{\partial f}{\partial x}\right|_{\mathbf{x}_i} = \sum_{j=1}^{m} \alpha_{i,j} f(\mathbf{x}_{i,j}) + \alpha_{i,m+1} f(\mathbf{x}_i) \qquad (1)$$

where $\alpha_{i,j}$ are the weighting coefficients. The reference point $\mathbf{x}_i$ does not belong to its supporting domain.

We combine this method with the local radial basis function (RBF) based interpolation of the function $f$. If $\varphi$ is a RBF and we consider the center point $\mathbf{x}_i$, we may write the interpolant to the function $f$ as

$$f(\mathbf{x}) = \sum_{j=1}^{m} \lambda_{i,j}\varphi(\|\mathbf{x}-\mathbf{x}_{i,j}\|,\epsilon) + \lambda_{i,m+1}\varphi(\|\mathbf{x}-\mathbf{x}_i\|,\epsilon) + \xi_i \qquad (2)$$

where $\lambda_{i,j}$ are the weighting coefficients, $\epsilon$ is the shape parameter, $\|\cdot\|$ is the Euclidian norm and $\xi_i$ is a constant polynomial term.

Concerning to the coefficient $\lambda_{i,m+1}$ we impose the condition

$$\lambda_{i,m+1} = -\sum_{j=1}^{m} \lambda_{i,j} \qquad (3)$$

Substituting condition (3) into Eq. (2) we obtain

$$f(\mathbf{x}) = \sum_{j=1}^{m} \lambda_{i,j} g_{i,j}(\mathbf{x}) + \xi_i \qquad (4)$$

where

$$g_{i,j}(\mathbf{x}) = \varphi(\|\mathbf{x}-\mathbf{x}_{i,j}\|,\epsilon) - \varphi(\|\mathbf{x}-\mathbf{x}_i\|,\epsilon), \quad j = 1,\ldots,m \qquad (5)$$

From Eq. (4) it is easy to compute the partial derivatives of the function $f$ if we know the partial derivatives of the functions $g_{i,j}$. For example,

$$\left.\frac{\partial f}{\partial x}\right|_{\mathbf{x}_i} = \sum_{j=1}^{m} \lambda_{i,j} \left.\frac{\partial g_{i,j}}{\partial x}\right|_{\mathbf{x}_i} \qquad (6)$$

Now we determine the partial derivatives of the functions $g_{i,j}$ by solving the following $m + 1$ equations with respect to $m + 1$ weighting coefficients $\alpha_{i,j}$:

$$\left.\frac{\partial g_{i,j}}{\partial x}\right|_{\mathbf{x}_i} = \sum_{k=1}^{m} \alpha_{i,k} g_{i,j}(\mathbf{x}_{i,k}) + \alpha_{i,m+1} g_{i,j}(\mathbf{x}_i), \quad j = 1,\ldots,m \qquad (7)$$

$$\sum_{k=1}^{m} \alpha_{i,k} + \alpha_{i,m+1} = 0 \qquad (8)$$

With this formulation we just need the information of positions of the scattered points in the domain to discretize the derivatives of function $f$. We use a support distance ($dmax$) to define the support domain of each point $\mathbf{x}_i$ of the domain of the function $f$.

## 3. The Murakami's Zig-Zag function

Let us consider a laminated plate composed of perfectly bonded layers, being $z$ the thickness coordinate of the whole plate while $z_k$ is the layer thickness coordinate. $a$ and $h$ are length and thickness of the square laminated plate, respectively. The adimensional layer coordinate $\zeta_k = (2z_k)/h_k$ is further introduced ($h_k$ is the thickness of the $k$th layer). The Murakami's Zig-Zag function $Z(z)$ was defined according to the following formula [17]

$$Z(z) = (-1)^k \zeta_z \tag{9}$$

$Z(z)$ has the following properties:

(1) It is a piece-wise linear function of layer coordinates $z_k$,
(2) $Z(z)$ has unit amplitude for the whole layers,
(3) the slope $Z'(z) = \frac{dZ}{dz}$ assumes opposite sign between two-adjacent layers. Its amplitude is layer thickness independent.

Here, we use the Murakami's original ZZF, for which the following displacement field is defined as:

$$u = u_0 + zu_1 + (-1)^k \frac{2}{h_k}\left(z - \frac{1}{2}(z_k + z_{k+1})\right)u_Z \tag{10}$$

$$v = v_0 + zv_1 + (-1)^k \frac{2}{h_k}\left(z - \frac{1}{2}(z_k + z_{k+1})\right)v_Z \tag{11}$$

$$w = w_0 + zw_1 + (-1)^k \frac{2}{h_k}\left(z - \frac{1}{2}(z_k + z_{k+1})\right)w_Z \tag{12}$$

where $z_k$, $z_{k+1}$ are the bottom and top $z$-coordinates at each layer. The additional degrees of freedom $u_Z$, $v_Z$ have a meaning of displacement, and its amplitude is layer independent the generalized displacements $u_1$, $v_1$ have similar meanings as first-order rotations of the normal to the middle-surface of the plate.

## 4. The unified formulation

The unified formulation (UF) proposed by Carrera [19,28–30], also known as CUF, is a powerful framework for the analysis of beams, plates and shells. The salient feature of CUF is the unified manner in which all considered variables (displacements and stresses) can be treated. This formulation has been applied in several finite element analysis, either using the Principle of Virtual Displacements, or by using the Reissner's Mixed Variational theorem. The stiffness matrix components, the external force terms or the inertia terms can be obtained directly with this UF, irrespective of the shear deformation theory being considered.

In this section, the fundamental nuclei are obtained by means of the Carrera's unified formulation. These allow the derivation of the equations of motion and boundary conditions, in weak form for the finite element analysis; and in strong form for the present RBF collocation.

### 4.1. Governing equations and boundary conditions in the framework of unified formulation

If a multi-layered plate with $N_l$ layers is considered, the Principle of Virtual Displacements (PVD) for the pure-mechanical case reads:

$$\sum_{k=1}^{N_l} \int_{\Omega_k} \int_{A_k} \left\{ \delta \boldsymbol{\epsilon}_{pG}^{k\ T} \boldsymbol{\sigma}_{pC}^k + \delta \boldsymbol{\epsilon}_{nG}^{k\ T} \boldsymbol{\sigma}_{nC}^k \right\} d\Omega_k dz = \sum_{k=1}^{N_l} \delta L_e^k \tag{13}$$

where $\Omega_k$ and $A_k$ are the integration domains in plane $(x,y)$ and $z$ direction, respectively. Here, $k$ indicates the layer and $T$ the transpose of a vector, and $\delta L_e^k$ is the external work for the $k$th layer. $G$ means geometrical relations and $C$ constitutive equations.

The steps to obtain the governing equations are:

- Substitution of the geometrical relations (subscript G).
- Substitution of the appropriate constitutive equations (subscript C).
- Introduction of the unified formulation.

Stresses and strains are separated into in-plane and normal components, denoted respectively by the subscripts $p$ and $n$. The mechanical strains in the $k$th layer can be related to the displacement field $\mathbf{u}^k = \left\{u_x^k, u_y^k, u_z^k\right\}$ via the geometrical relations:

$$\begin{aligned} \boldsymbol{\epsilon}_{pG}^k &= [\epsilon_{xx}, \epsilon_{yy}, \gamma_{xy}]^{kT} = \mathbf{D}_p \mathbf{u}^k \\ \boldsymbol{\epsilon}_{nG}^k &= [\gamma_{xz}, \gamma_{yz}, \epsilon_{zz}]^{kT} = (\mathbf{D}_{np} + \mathbf{D}_{nz})\ \mathbf{u}^k \end{aligned} \tag{14}$$

wherein the differential operator arrays are defined as follows:

$$\mathbf{D}_p = \begin{bmatrix} \partial_x & 0 & 0 \\ 0 & \partial_y & 0 \\ \partial_y & \partial_x & 0 \end{bmatrix}, \quad \mathbf{D}_{np} = \begin{bmatrix} 0 & 0 & \partial_x \\ 0 & 0 & \partial_y \\ 0 & 0 & 0 \end{bmatrix}, \quad \mathbf{D}_{nz} = \begin{bmatrix} \partial_z & 0 & 0 \\ 0 & \partial_z & 0 \\ 0 & 0 & \partial_z \end{bmatrix} \tag{15}$$

The 3D constitutive equations are given as:

$$\begin{aligned} \boldsymbol{\sigma}_{pC}^k &= \mathbf{C}_{pp}^k \boldsymbol{\epsilon}_{pG}^k + \mathbf{C}_{pn}^k \boldsymbol{\epsilon}_{nG}^k \\ \boldsymbol{\sigma}_{nC}^k &= \mathbf{C}_{np}^k \boldsymbol{\epsilon}_{pG}^k + \mathbf{C}_{nn}^k \boldsymbol{\epsilon}_{nG}^k \end{aligned} \tag{16}$$

with

$$\begin{aligned} \mathbf{C}_{pp}^k &= \begin{bmatrix} C_{11}^k & C_{12}^k & C_{16}^k \\ C_{12}^k & C_{22}^k & C_{26}^k \\ C_{16}^k & C_{26}^k & C_{66}^k \end{bmatrix} \quad \mathbf{C}_{pn}^k = \begin{bmatrix} 0 & 0 & C_{13}^k \\ 0 & 0 & C_{23}^k \\ 0 & 0 & C_{36}^k \end{bmatrix} \\ \mathbf{C}_{np}^k &= \begin{bmatrix} 0 & 0 & 0 \\ 0 & 0 & 0 \\ C_{13}^k & C_{23}^k & C_{36}^k \end{bmatrix} \quad \mathbf{C}_{nn}^k = \begin{bmatrix} C_{55}^k & C_{45}^k & 0 \\ C_{45}^k & C_{44}^k & 0 \\ 0 & 0 & C_{33}^k \end{bmatrix} \end{aligned} \tag{17}$$

According to the unified formulation by Carrera, the three displacement components $u_x^k$, $u_y^k$ and $u_z^k$ and their relative variations can be modelled as:

$$\begin{aligned} \left(u_x^k, u_y^k, u_z^k\right) &= F_\tau \left(u_{x\tau}^k, u_{y\tau}^k, u_{z\tau}^k\right) \quad \left(\delta u_x^k, \delta u_y^k, \delta u_z^k\right) \\ &= F_s \left(\delta u_{xs}^k, \delta u_{ys}^k, \delta u_{zs}^k\right) \end{aligned} \tag{18}$$

where $F_\tau$ and $F_s$ can be general functions of the thickness coordinate $z$. A Taylor expansion from first up to 4th order: $F_0 = z^0 = 1$, $F_1 = z^1 = z, \ldots, F_N = z^N, \ldots, F_4 = z^4$ is taken if an Equivalent Single Layer (ESL) approach is used.

Substituting the geometrical relations, the constitutive equations and the unified formulation into the variational statement PVD, for the $k$th layer, one obtains the governing equations for a multi-layered plate subjected to mechanical loadings:

$$\delta \mathbf{u}_s^{k^T} : \mathbf{K}_{uu}^{k\tau s} \mathbf{u}_\tau^k = \mathbf{P}_{u\tau}^k \tag{19}$$

and the corresponding Neumann-type boundary conditions on $\Gamma_k$:

$$\boldsymbol{\Pi}_d^{k\tau s} \mathbf{u}_\tau^k = \boldsymbol{\Pi}_d^{k\tau s} \bar{\mathbf{u}}_\tau^k, \tag{20}$$

where $\mathbf{K}_{uu}^{k\tau s}$ and $\boldsymbol{\Pi}_d^{k\tau s}$ are the fundamental nuclei and $\mathbf{P}_{u\tau}^k$ are variationally consistent loads with applied pressure. The explicit forms of the fundamental nuclei are given in Appendix A. For more details about the mathematical passages to obtain the governing equations and boundary conditions one can refer to [23].

### 4.2. Dynamic governing equations

The PVD for the dynamic case is expressed as:

$$\begin{aligned} &\sum_{k=1}^{N_l} \int_{\Omega_k} \int_{A_k} \left\{ \delta \boldsymbol{\epsilon}_{pG}^{k\ T} \boldsymbol{\sigma}_{pC}^k + \delta \boldsymbol{\epsilon}_{nG}^{k\ T} \boldsymbol{\sigma}_{nC}^k \right\} d\Omega_k dz \\ &\quad = \sum_{k=1}^{N_l} \int_{\Omega_k} \int_{A_k} \rho^k \delta \mathbf{u}^{kT} \ddot{\mathbf{u}}^k d\Omega_k dz + \sum_{k=1}^{N_l} \delta L_e^k \end{aligned} \tag{21}$$

**Table 1**
[0°/90°/90°/0°] square laminated plate under zig-zag formulation.

| $\frac{a}{h}$ | Method | $\bar{w}$ | $\bar{\sigma}_{xx}$ | $\bar{\sigma}_{yy}$ | $\bar{\tau}_{zx}$ | $\bar{\tau}_{xy}$ |
|---|---|---|---|---|---|---|
| 4 | HSDT [31] | 1.8937 | 0.6651 | 0.6322 | 0.2064 | 0.0440 |
| | FSDT [32] | 1.7100 | 0.4059 | 0.5765 | 0.1398 | 0.0308 |
| | Elasticity [33] | 1.954 | 0.720 | 0.666 | 0.270 | 0.0467 |
| | RBF-FD-CUF [24] | 1.8931 | 0.6408 | 0.8506 | 0.2160 | 0.0436 |
| | Present (13 × 13 grid) | 1.8941 | 0.6408 | 0.8507 | 0.2162 | 0.0437 |
| | Present (17 × 17 grid) | 1.8925 | 0.6406 | 0.8504 | 0.2160 | 0.0689 |
| | Present (21 × 21 grid) | 1.8932 | 0.6408 | 0.8506 | 0.2160 | 0.0436 |
| | Present (25 × 25 grid) | 1.8931 | 0.6408 | 0.8506 | 0.2160 | 0.0436 |
| 10 | HSDT [31] | 0.7147 | 0.5456 | 0.3888 | 0.2640 | 0.0268 |
| | FSDT [32] | 0.6628 | 0.4989 | 0.3615 | 0.1667 | 0.0241 |
| | Elasticity [33] | 0.743 | 0.559 | 0.403 | 0.301 | 0.0276 |
| | RBF-FD-CUF [24] | 0.7227 | 0.5460 | 0.4194 | 0.2978 | 0.0269 |
| | Present (13 × 13 grid) | 0.7239 | 0.5466 | 0.4198 | 0.2985 | 0.0270 |
| | Present (17 × 17 grid) | 0.7221 | 0.5456 | 0.4191 | 0.2976 | 0.0269 |
| | Present (21 × 21 grid) | 0.7228 | 0.5461 | 0.4194 | 0.2979 | 0.0269 |
| | Present (25 × 25 grid) | 0.7227 | 0.5460 | 0.4194 | 0.2978 | 0.0269 |
| 100 | HSDT [31] | 0.4343 | 0.5387 | 0.2708 | 0.2897 | 0.0213 |
| | FSDT [32] | 0.4337 | 0.5382 | 0.2705 | 0.1780 | 0.0213 |
| | Elasticity [33] | 0.4347 | 0.539 | 0.271 | 0.339 | 0.0214 |
| | RBF-FD-CUF [24] | 0.4294 | 0.5364 | 0.2699 | 0.3345 | 0.0211 |
| | Present (13 × 13 grid) | 0.5248 | 0.6560 | 0.3650 | 0.4145 | 0.0253 |
| | Present (17 × 17 grid) | 0.4077 | 0.5101 | 0.2590 | 0.3173 | 0.0200 |
| | Present (21 × 21 grid) | 0.4350 | 0.5430 | 0.2726 | 0.3388 | 0.0214 |
| | Present (25 × 25 grid) | 0.4303 | 0.5374 | 0.2704 | 0.3352 | 0.0212 |

where $\rho^k$ is the mass density of the $k$th layer and double dots denote acceleration.

By substituting the geometrical relations, the constitutive equations and the unified formulation, we obtain the following governing equations:

$$\delta \mathbf{u}_s^{k^T} : \mathbf{K}_{uu}^{k\tau s}\mathbf{u}_\tau^k = -\mathbf{M}^{k\tau s}\ddot{\mathbf{u}}_\tau^k + \mathbf{P}_{u\tau}^k \quad (22)$$

In the case of free vibrations one has:

$$\delta \mathbf{u}_s^{k^T} : \mathbf{K}_{uu}^{k\tau s}\mathbf{u}_\tau^k = -\mathbf{M}^{k\tau s}\ddot{\mathbf{u}}_\tau^k \quad (23)$$

where $\mathbf{M}^{k\tau s}$ is the fundamental nucleus for the inertial term. For the explicit expression of $\mathbf{M}^{k\tau s}$, see Appendix A.

The geometrical and mechanical boundary conditions for the dynamic problem are the same of the static case.

Resorting to the displacement field in Eqs. (21)–(23), we choose vectors $F_\tau,\ F_s = \left[1\ z\ (-1)^k \frac{2}{h_k}\left(z - \frac{1}{2}(z_k + z_{k+1})\right)\right]$ for displacements $u,\ v$, and $F_\tau,\ F_s = [1\ z\ z^2]$ for displacement $w$. We then obtain all terms of the equations of motion by integrating through the thickness direction.

It is interesting to note that under this combination of the Unified Formulation and RBF collocation, the collocation code depends only on the choice of $F_\tau$, $F_s$, in order to solve this type of problems. We designed a MATLAB code that just by changing $F_\tau$, $F_s$ can analyse static deformations, free vibrations and buckling loads for any type of $C^\circ$ shear deformation theory. An obvious advantage of the present methodology is that the tedious and time-consuming derivation of the equations of motion and boundary conditions for a particular shear deformation theory is no longer a problem.

## 5. Numerical examples

In all following examples a Chebyshev grid was used. The Wendland function used in all examples is defined as

$$\phi(r) = (1 - c\ r)_+^8 (32(c\ r)^3 + 25(c\ r)^2 + 8c\ r + 1) \quad (24)$$

where the shape parameter ($c$) is given by $c = 2/\sqrt{N}$, being $N$ the number of points in one coordinate direction. We always consider a plate with side $a = 2$, and a local support distance $d_{max} = 1.5$.

### 5.1. Static problems-cross-ply laminated plates

A simply supported square laminated plate of side $a$ and thickness $h$ is composed of four equally layers oriented at [0°/90°/90°/0°]. The plate is subjected to a sinusoidal vertical pressure of the form

$$p_z = P \sin\left(\frac{\pi x}{a}\right) \sin\left(\frac{\pi y}{a}\right)$$

with the origin of the coordinate system located at the lower left corner on the midplane and $P$ the maximum load (at center of plate).

The orthotropic material properties for each layer are

$$E_1 = 25.0E_2 \quad G_{12} = G_{13} = 0.5E_2 \quad G_{23} = 0.2E_2 \quad \nu_{12} = 0.25$$

The in-plane displacements, the transverse displacements, the normal stresses and the in-plane and transverse shear stresses are presented in normalized form as

$$\bar{w} = \frac{10^2 w_{(a/2,a/2,0)} h^3 E_2}{P a^4} \quad \bar{\sigma}_{xx} = \frac{\sigma_{xx(a/2,a/2,h/2)} h^2}{P a^2} \quad \bar{\sigma}_{yy} = \frac{\sigma_{yy(a/2,a/2,h/4)} h^2}{P a^2}$$

$$\bar{\tau}_{xz} = \frac{\tau_{xz(0,a/2,0)} h}{P a} \quad \bar{\tau}_{xy} = \frac{\tau_{xy(0,0,h/2)} h^2}{P a^2}$$

In Table 1 we present results for the present ZZ theory, using 13 × 13 up to 25 × 25 points. We compare results with higher-order analytical solutions by Reddy [31], FSDT analytical solutions by Reddy and Chao [32], and an exact (analytical) solution by Pagano [33]. We also compare with a local RBF-FD (Finite Differences) technique by the authors [24]. Our ZZ theory produces excellent results, when compared with other HSDT theories, for all $a/h$ ratios, for transverse displacements, normal stresses and transverse shear stresses. It can be seen that the present technique matches the RBF-FD closely. Note that the transverse shear stresses are obtained directly from the constitutive equations.

### 5.2. Free vibration problems-cross-ply laminated plates

In this example, all layers of the laminate are assumed to be of the same thickness, density and made of the same linearly elastic

**Table 2**
The normalized fundamental frequency of the simply-supported cross-ply laminated square plate [0°/90°/90°/0°] ($\bar{w} = (wa^2/h)\sqrt{\rho/E_2},\ h/a = 0.2$).

| Method | Grid | $E_1/E_2$ | | | |
|---|---|---|---|---|---|
| | | 10 | 20 | 30 | 40 |
| Liew [35] | | 8.2924 | 9.5613 | 10.320 | 10.849 |
| Exact (Reddy, Khdeir) [15,34] | | 8.2982 | 9.5671 | 10.326 | 10.854 |
| RBF-FD-CUF [24] | | 8.4142 | 9.6629 | 10.4013 | 10.9054 |
| Present ($\nu_{23}$ = 0.25) | 13 × 13 | 8.4089 | 9.6586 | 10.3974 | 10.9017 |
| | 17 × 17 | 8.4168 | 9.6651 | 10.4033 | 10.9073 |
| | 21 × 21 | 8.4136 | 9.6624 | 10.4009 | 10.9050 |

**Table 3**
Uni-axial buckling load of four-layer [0°/90°/90°/0°] simply supported laminated plate ($\overline{N} = \overline{N}_{xx}a^2/(E_2h^3),\ \overline{N}_{xy} = 0,\ \overline{N}_{yy} = 0$).

| Grid | Present | RBF-FD-CUF [24] | Liew et al. [37] | Khdeir and Librescu [36] |
|---|---|---|---|---|
| 13 × 13 | 23.7805 | 23.8110 | 23.463 | 23.453 |
| 17 × 17 | 23.8261 | | | |
| 21 × 21 | 23.8077 | | | |

composite material. The following material parameters of a layer are used:

$$\frac{E_1}{E_2} = 10, 20, 30 \text{ or } 40; \quad G_{12} = G_{13} = 0.6E_2; \quad G_3 = 0.5E_2;$$
$$\nu_{12} = 0.25$$

The subscripts 1 and 2 denote the directions normal and transverse to the fiber direction in a lamina, which may be oriented at an angle to the plate axes. The ply angle of each layer is measured from the global x-axis to the fiber direction.

The example considered is a simply supported square plate of the cross-ply lamination [0°/90°/90°/0°]. The thickness and length of the plate are denoted by $h$ and $a$, respectively. The thickness-to-span ratio $h/a$ = 0.2 is employed in the computation. Table 2 lists the fundamental frequency of the simply supported laminate made of various modulus ratios of $E_1/E_2$. Three grids of 13 × 13 to 21 × 21 points are considered. Although the present approach considers a thickness-stretching component, results are compared with two theories with no thickness-stretching component, [15,34 and 35]. Therefore in these two cases some differences in results are expectable. Still, it is found that the present meshless results are in agreement with the values of Reddy and Khdeir and the meshfree results of Liew based on the FSDT. We also compare with a local RBF-FD (Finite Differences) technique by the authors [24], and show that both techniques present similar results.

*5.3. Buckling examples*

Three-layer [0°/90°/0°] and four-layer [0°/90°/90°0°] square cross-ply laminates are chosen to compute the uni- and bi-axial buckling loads. The plate has width $a$ and thickness $h$. The span-to-thickness ratio $a/h$ is taken to be 10. Three grids of 13 × 13 to 21 × 21 points are considered. All layers are assumed to be of the same thickness and material properties:

$$E_1/E_2 = 40; \quad G_{12}/E_2 = G_{13}/E_2 = 0.6; \quad G_{23}/E_2 = 0.5; \quad \nu_{12} = 0.25$$

Table 3 lists the uni-axial buckling loads of the four-layer simply supported laminated plate. Exact (analytical) solutions by Khdeir and Librescu [36] and differential quadrature results by Liew et al. [37] based on the FSDT are also presented for comparison. It is found that the critical buckling load is obtained with a few grid points. The present results are in excellent correlation with those of Khdeir and Librescu [36], and those of Liew et al. [37]. Fig. 2 shows the first 4 buckling modes, for uni-axial buckling load of four-layer [0°/90°/90°/0°] simply supported laminated plate ($\overline{N} = \overline{N}_{xx}a^2/(E_2h^3), \overline{N}_{xy} = 0, \overline{N}_{yy} = 0$), using a grid of 13 × 13 points. We also compare with a local RBF-FD (Finite Differences) technique by the authors [24], and show that results by both techniques are similar.

Table 4 tabulates the bi-axial buckling loads of the [0°/90°/0°] laminated plate. The laminated plate is simply supported along the edges parallel to the $x$-axis while the other two edges may be simply supported (S), or clamped (C). The notations SS, SC, and CC refer to the boundary conditions of the two edges parallel to the $x$-axis only.

In Fig. 3 it is illustrated the first 4 buckling modes for bi-axial buckling load of three-layer [0°/90°/0°] simply supported laminated plate ($\overline{N} = \overline{N}_{xx}a^2/(E_2h^3),\ \overline{N}_{xy} = 0,\ \overline{N}_{yy} = \overline{N}_{xx}$), using a grid of 17 × 17 points.

In Fig. 4 it is illustrated the first 4 buckling modes for bi-axial buckling load of three-layer [0°/90°/0°] SCSC laminated plate ($\overline{N} = \overline{N}_{xx}a^2/(E_2h^3),\ \overline{N}_{xy} = 0,\ \overline{N}_{yy} = \overline{N}_{xx}$), using a grid of 17 × 17 points.

In Fig. 5 it is illustrated the first 4 buckling modes for bi-axial buckling load of three-layer [0°/90°/0°] SSSC laminated plate ($\overline{N} = \overline{N}_{xx}a^2/(E_2h^3),\ \overline{N}_{xy} = 0,\ \overline{N}_{yy} = \overline{N}_{xx}$), using a grid of 17 × 17 points.

It is found that excellent agreement is achieved for all edge conditions when comparing the results obtained by the present LRBFDQ approach with the FSDT solutions by Khdeir and Librescu [36], and MLSDQ solutions of Liew et al. [37]. Note that although comparison with other sources are excellent, the critical loads are related to the second mode (SSSS), fourth mode (SCSC) and third mode (SSSC).

*5.4. Comparing with 3D solutions*

In order to compare with existing 3D solutions, static deformations and free vibrations are obtained for the Srinivas and Rao 3D results [25]. Both static and free vibrations results use the following material properties (see [25] for more details):

$$E_y/E_x = 0.543103; \quad E_{xy}/E_x = 0.23319; \quad E_z/E_x = 0.530171;$$
$$E_{xz}/E_x = 0.10776; \quad E_{yz}/E_x = 0.98276;$$
$$G_{xy}/E_x = 0.262931; \quad G_{xz}/E_x = 0.159914; \quad G_{yz}/E_x = 0.26681 \tag{25}$$

The static problem considers a simply-supported plate under uniform load $q_0$, side-to-thickness ratio $a/h$ = 10. A three-layer laminate

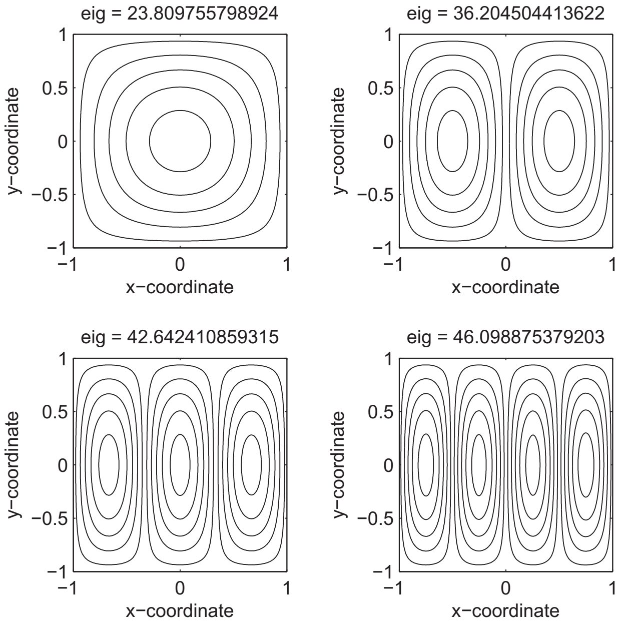


**Fig. 2.** First 4 buckling modes: uni-axial buckling load of four-layer [0°/90°/90°/0°] simply supported laminated plate $(\overline{N} = \overline{N}_{xx}a^2/(E_2h^3),\ \overline{N}_{xy} = 0,\ \overline{N}_{yy} = 0)$, grid $17 \times 17$ points.

**Table 4**
Bi-axial buckling load of three-layer [0°/90°/0°] simply supported laminated plate $(\overline{N} = \overline{N}_{xx}a^2/(E_2h^3),\ \overline{N}_{xy} = 0,\ \overline{N}_{yy} = \overline{N}_{xx})$.

| Grid | SS | SC | CC |
|---|---|---|---|
| $13 \times 13$ | 10.1882 | 11.7608 | 13.6766 |
| $17 \times 17$ | 10.1905 | 11.7526 | 13.6594 |
| $21 \times 21$ | 10.1912 | 11.7564 | 13.6633 |
| RBF-FD-CUF [24] | 10.1907 | 11.7557 | 13.6629 |
| Liew et al. [37] | 10.178 | 11.575 | 13.260 |
| Khdeir and Librescu [36] | 10.202 | 11.602 | 13.290 |

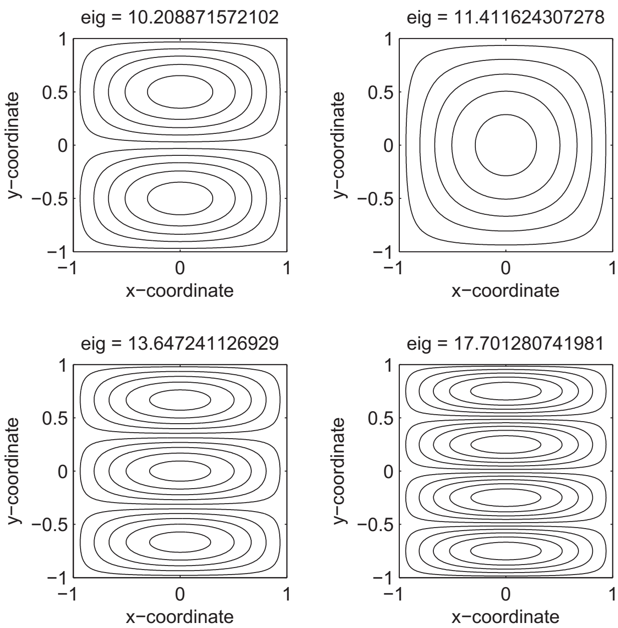


**Fig. 3.** First 4 buckling modes: bi-axial buckling load of three-layer [0°/90°/0°] simply supported (SSSS) laminated plate $(\overline{N} = \overline{N}_{xx}a^2/(E_2h^3),\ \overline{N}_{xy} = 0,\ \overline{N}_{yy} = \overline{N}_{xx})$, grid $17 \times 17$ points.

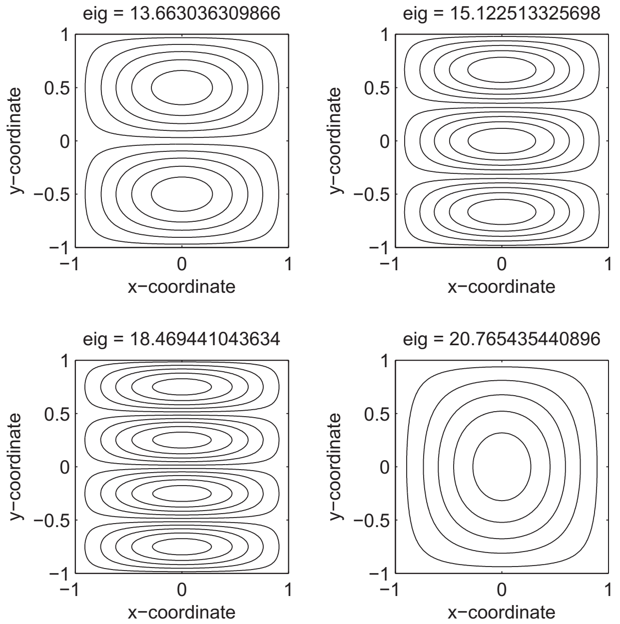


**Fig. 4.** First 4 buckling modes: bi-axial buckling load of three-layer [0°/90°/0°] SCSC laminated plate $(\overline{N} = \overline{N}_{xx}a^2/(E_2h^3),\ \overline{N}_{xy} = 0,\ \overline{N}_{yy} = \overline{N}_{xx})$, grid $17 \times 17$ points.

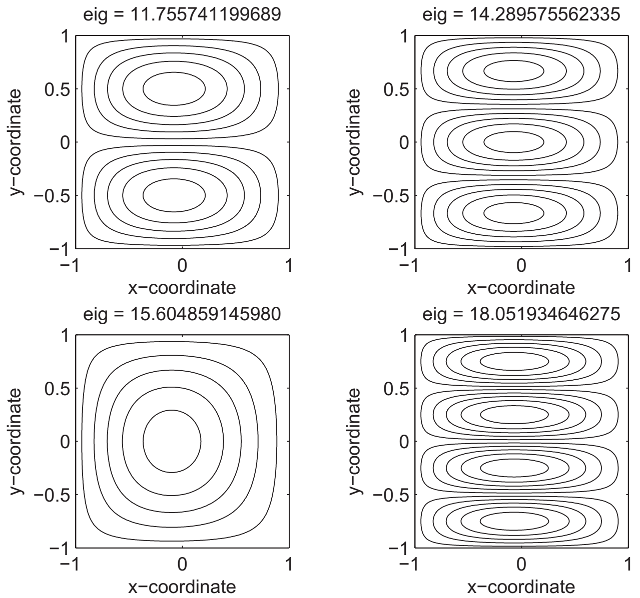


**Fig. 5.** First 4 buckling modes: bi-axial buckling load of three-layer [0°/90°/0°] SSSC laminated plate $(\overline{N} = \overline{N}_{xx}a^2/(E_2h^3),\ \overline{N}_{xy} = 0,\ \overline{N}_{yy} = \overline{N}_{xx})$, grid $17 \times 16$ points.

**Table 5**
Central deflections (normalized by $E_{x_2}/hq_0$, $E_{x_2}$-elastic modulus of mid-ply) for a square simply-supported three-ply laminate subject to uniform loading.

| $\beta$ | 1 | 5 | 10 | 15 |
|---|---|---|---|---|
| present ($13 \times 13$) | 678.65 | 252.43 | 154.98 | 117.98 |
| present ($17 \times 17$) | 687.94 | 256.11 | 157.80 | 120.56 |
| present ($21 \times 21$) | 687.92 | 256.15 | 157.92 | 120.75 |
| Liew et al. [26] | 690.96 | 260.38 | 160.43 | 122.61 |
| Srinivas and Rao [25] | 688.58 | 258.97 | 159.38 | 121.73 |
| Error (%) | 0.10 | 1.09 | 0.92 | 0.81 |

is considered with skin thicknesses $h/10$ and core thickness $8h/10$. The skin material properties are obtained by multiplying the core

**Table 6**
Non-dimensionalized frequencies (normalized by $\lambda = \omega h\sqrt{\rho/E_{2x}}$) of simply-supported square sandwich laminates.

| $\beta = E_{1x}/E_{2x}$ | Method | $\lambda_1$ | $\lambda_2$ | $\lambda_3$ | $\lambda_4$ |
|---|---|---|---|---|---|
| 1 | Present (13 × 13) | 0.047729 | 0.103480 | 0.117547 | 0.162313 |
| | Present (17 × 17) | 0.047446 | 0.103468 | 0.117455 | 0.162267 |
| | Present (21 × 21) | 0.047451 | 0.103459 | 0.117449 | 0.162272 |
| | Zhang et al. [27] | 0.047338 | 0.10313 | 0.11850 | 0.16109 |
| | Srinivas and Rao [25] | 0.047419 | – | – | – |
| 2 | Present (13 × 13) | 0.057783 | 0.124692 | 0.140518 | 0.177806 |
| | Present (17 × 17) | 0.057426 | 0.124686 | 0.140409 | 0.177754 |
| | Present (21 × 21) | 0.057434 | 0.124673 | 0.140402 | 0.177760 |
| | Zhang et al. [27] | 0.056917 | 0.12304 | 0.13931 | 0.17644 |
| | Srinivas and Rao [25] | 0.057041 | – | – | – |
| 5 | Present (13 × 13) | 0.078041 | 0.164835 | 0.178935 | 0.217767 |
| | Present (17 × 17) | 0.077593 | 0.164841 | 0.178814 | 0.217703 |
| | Present (21 × 21) | 0.077607 | 0.164825 | 0.178807 | 0.217711 |
| | Zhang et al. [27] | 0.076936 | 0.16294 | 0.17770 | 0.21585 |
| | Srinivas and Rao [25] | 0.077148 | – | – | – |
| 10 | Present (13 × 13) | 0.099227 | 0.203694 | 0.211934 | 0.271602 |
| | Present (17 × 17) | 0.098582 | 0.203749 | 0.211795 | 0.271524 |
| | Present (21 × 21) | 0.098605 | 0.203728 | 0.211788 | 0.271533 |
| | Zhang et al. [27] | 0.097783 | 0.20169 | 0.21049 | 0.26845 |
| | Srinivas and Rao [25] | 0.098104 | – | – | – |

properties by a scalar $\beta$. In Table 5 we compare the present solution with the exact solution by Srinivas and Rao [25], and a differential quadrature technique by Liew et al. [26]. The errors with respect to the exact solution are below 1% for all cases.

The free vibration problem considers again a simply-supported plate, side-to-thickness ratio $a/h = 10$. A three-layer laminate is considered with skin thicknesses $h/10$ and core thickness $8h/10$. The skin material properties are obtained by multiplying the core properties by a scalar $\beta$. In Table 6 we compare the present solution with the exact solution by Srinivas and Rao [25], and a differential quadrature technique by Zhang et al. [27]. The present solution matches the exact solution with errors in the 0.1% range.

## 6. Conclusions

In this paper we presented a study using the LRBFDQ collocation method to analyse static deformations, free vibrations and buckling loads of thin and thick laminated plates using Murakami's Zig-Zag function, allowing for through-the-thickness deformations.This has not been done before and fills the gap of knowledge in this research area.

Using the unified formulation with the radial basis collocation, all the $C^o$ plate formulations can be easily discretized by LRBFDQ collocation.

We analysed square cross-ply laminated plates in bending, free vibrations and buckling loads. The present results were compared with existing analytical solutions or finite element, 3D and RBF-FD meshless solutions and excellent agreement was observed in all cases. No special advantages or disadvantages are found between RBF-FD and RBF-DQ methods, for these type of problems.


## Acknowledgement

The support of Ministério da Ciência Tecnologia e do Ensino superior and Fundo Social Europeu (MCTES and FSE) under programs POPH-QREN and project PTDC/EME-PME/109116/2008 are gratefully acknowledged.


## Appendix A

The explicit expressions of fundamental nuclei for the equations of motion and boundary conditions, in weak form for the RBF collocation, are listed below:

$$
\begin{aligned}
K_{uu_{11}}^{k\tau s} &= -F_sF_\tau C_{11}^k\partial_x^s\partial_x^\tau - F_sF_\tau C_{16}^k\partial_x^s\partial_y^\tau + F_{s,z}F_{\tau,z}C_{55}^k - F_sF_\tau C_{16}^k\partial_y^s\partial_x^\tau \\
&\quad - F_sF_\tau C_{66}^k\partial_y^s\partial_y^\tau \\
K_{uu_{12}}^{k\tau s} &= -F_sF_\tau C_{12}^k\partial_x^s\partial_y^\tau - F_sF_\tau C_{16}^k\partial_x^s\partial_x^\tau + F_{s,z}F_{\tau,z}C_{45}^k - F_sF_\tau C_{26}^k\partial_y^s\partial_y^\tau \\
&\quad - F_sF_\tau C_{66}^k\partial_y^s\partial_x^\tau \\
K_{uu_{13}}^{k\tau s} &= -F_sF_{\tau,z}C_{13}^k\partial_x^s - F_sF_{\tau,z}C_{36}^k\partial_y^s + F_{s,z}F_\tau C_{45}^k\partial_y^\tau \\
&\quad + F_{s,z}F_\tau C_{55}^k\partial_x^\tau \\
K_{uu_{21}}^{k\tau s} &= -F_sF_\tau C_{12}^k\partial_y^s\partial_x^\tau - F_sF_\tau C_{26}^k\partial_y^s\partial_y^\tau + F_{s_z}F_{\tau_z}C_{45}^k - F_sF_\tau\partial_x^s\partial_x^\tau C_{16}^k \\
&\quad - F_sF_\tau C_{66}^k\partial_x^s\partial_y^\tau \\
K_{uu_{22}}^{k\tau s} &= -F_sF_\tau C_{22}^k\partial_y^s\partial_y^\tau - F_sF_\tau C_{26}^k\partial_y^s\partial_x^\tau + F_{s_z}F_{\tau_z}C_{44}^k - F_sF_\tau C_{26}^k\partial_x^s\partial_y^\tau \\
&\quad - F_sF_\tau C_{66}^k\partial_x^s\partial_x^\tau \\
K_{uu_{23}}^{k\tau s} &= -F_sF_{\tau_z}C_{23}^k\partial_y^s - F_sF_{\tau_z}C_{36}^k\partial_x^s + F_{s_z}F_\tau C_{44}^k\partial_y^\tau \\
&\quad + F_{s_z}F_\tau C_{45}^k\partial_x^\tau \\
K_{uu_{31}}^{k\tau s} &= F_{s_z}F_\tau C_{13}^k\partial_x^\tau + F_{s_z}F_\tau C_{36}^k\partial_y^\tau - F_sF_{\tau_z}C_{45}^k\partial_y^s \\
&\quad - F_sF_{\tau_z}C_{55}^k\partial_x^s \\
K_{uu_{32}}^{k\tau s} &= F_{s_z}F_\tau C_{23}^k\partial_y^\tau + F_{s_z}F_\tau C_{36}^k\partial_x^\tau - F_sF_{\tau_z}C_{44}^k\partial_y^s \\
&\quad - F_sF_{\tau_z}C_{45}^k\partial_x^s \\
K_{uu_{33}}^{k\tau s} &= F_{s_z}F_{\tau_z}C_{33}^k - F_sF_\tau C_{44}^k\partial_y^s\partial_y^\tau - F_sF_\tau C_{45}^k\partial_y^s\partial_x^\tau - F_sF_\tau C_{45}^k\partial_x^s\partial_y^\tau \\
&\quad - F_sF_\tau C_{55}^k\partial_x^s\partial_x^\tau
\end{aligned} \tag{26}
$$

$$
\begin{aligned}
\Pi_{11}^{k\tau s} &= n_xF_\tau F_sC_{11}^k\partial_x^\tau + n_xF_\tau F_sC_{16}^k\partial_y^\tau + n_yF_\tau F_sC_{16}^k\partial_x^\tau + n_yF_\tau F_sC_{66}^k\partial_y^\tau \\
\Pi_{12}^{k\tau s} &= n_xF_\tau F_sC_{12}^k\partial_y^\tau + n_xF_\tau F_sC_{16}^k\partial_x^\tau + n_yF_\tau F_sC_{26}^k\partial_y^\tau + n_yF_\tau F_sC_{66}^k\partial_x^\tau \\
\Pi_{13}^{k\tau s} &= n_xF_{\tau_z}F_sC_{13}^k + n_yF_{\tau_z}F_sC_{36}^k \\
\Pi_{21}^{k\tau s} &= n_yF_\tau F_sC_{12}^k\partial_x^\tau + n_yF_\tau F_sC_{26}^k\partial_y^\tau + n_xF_\tau F_sC_{16}^k\partial_x^\tau + n_xF_\tau F_sC_{66}^k\partial_y^\tau \\
\Pi_{22}^{k\tau s} &= n_yF_\tau F_sC_{22}^k\partial_y^\tau + n_yF_\tau F_sC_{26}^k\partial_x^\tau + n_xF_\tau F_sC_{26}^k\partial_y^\tau + n_xF_\tau F_sC_{66}^k\partial_x^\tau \\
\Pi_{23}^{k\tau s} &= n_yF_{\tau_z}F_sC_{23}^k + n_xF_{\tau_z}F_sC_{36}^k \\
\Pi_{31}^{k\tau s} &= n_yF_{\tau_z}F_sC_{45}^k + n_xF_{\tau_z}F_sC_{55}^k \\
\Pi_{32}^{k\tau s} &= n_yF_{\tau_z}F_sC_{44}^k + n_xF_{\tau_z}F_sC_{45}^k \\
\Pi_{33}^{k\tau s} &= n_yF_\tau F_sC_{44}^k\partial_y^\tau + n_yF_\tau F_sC_{45}^k\partial_x^\tau + n_xF_\tau F_sC_{45}^k\partial_y^\tau + n_xF_\tau F_sC_{55}^k\partial_x^\tau
\end{aligned} \tag{27}
$$

where $\partial$ indicates the partial derivative and $(n_x, n_y)$ are the components of the normal $\hat{\mathbf{n}}$ to the boundary of domain $\Omega$, along the directions $x$ and $y$, respectively. The subscript $z$ indicates the partial derivative with respect to $z$.

In the dynamic case, the fundamental nucleus for the inertial term $\mathbf{M}^{k\tau s}$ is:

$$M_{11}^{k\tau s} = F_\tau F_s \rho^k; \qquad M_{12}^{k\tau s} = 0; \quad M_{13}^{k\tau s} = 0 \tag{28}$$

$$M_{21}^{k\tau s} = 0; \qquad M_{22}^{k\tau s} = F_\tau F_s \rho^k; \quad M_{23}^{k\tau s} = 0 \tag{29}$$

$$M_{31}^{k\tau s} = 0; \qquad M_{32}^{k\tau s} = 0; \quad M_{33}^{k\tau s} = F_\tau F_s \rho^k \tag{30}$$

## Appendix B

A complete set of differential operators that allow to solve the boundary problem by any strong-form-based formulation (e.g., pseudo-spectrals, analytical solutions, radial basis functions, and so on).

The governing equations can be detailed as:

$$\begin{bmatrix} L_{11} & \cdots & L_{19} \\ \cdots & \cdots & \cdots \\ L_{91} & \cdots & L_{99} \end{bmatrix} \begin{bmatrix} u_0 \\ u_1 \\ u_Z \\ v_0 \\ v_1 \\ v_Z \\ w_0 \\ w_1 \\ w_Z \end{bmatrix} = - \begin{bmatrix} M_{11} & \cdots & M_{19} \\ \cdots & \cdots & \cdots \\ M_{91} & \cdots & M_{99} \end{bmatrix} \begin{bmatrix} \ddot{u}_0 \\ \ddot{u}_1 \\ \ddot{u}_Z \\ \ddot{v}_0 \\ \ddot{v}_1 \\ \ddot{v}_Z \\ \ddot{w}_0 \\ \ddot{w}_1 \\ \ddot{w}_Z \end{bmatrix} + \begin{bmatrix} F_{u0} \\ F_{u1} \\ F_{uZ} \\ F_{v0} \\ F_{v1} \\ F_{vZ} \\ F_{w0} \\ F_{w1} \\ F_{wZ} \end{bmatrix} \tag{31}$$

Considering the fundamental nuclei $\mathbf{K}_{uu}^{k\tau s}$ and $\mathbf{M}^{k\tau s}$ obtained by the Carrera's unified formulation, the non-zero differential operators in matrix $\mathbf{L}$ and the non-zero mass terms in matrix $\mathbf{M}$ can be expressed as follows:

$$\begin{aligned} L_{ij} &= \sum_{k=1}^{N_l} \int_{z_k}^{z_{k+1}} \mathbf{K}_{uu_{mn}}^{k\tau s} dz \\ M_{ij} &= \sum_{k=1}^{N_l} \int_{z_k}^{z_{k+1}} \mathbf{M}_{mn}^{k\tau s} dz \end{aligned} \tag{32}$$

where $N_l$ is the number of layers, and

$$\begin{aligned} i &= (s+1) + (m-1) \times 3 \\ j &= (\tau+1) + (n-1) \times 3 \end{aligned} \tag{33}$$

with $m$, $n$ = 1,2,3 and $\tau$, $s$ = 0,1,2.

Remembering that $F_\tau, F_s = \left[1 \quad z \quad (-1)^k \frac{2}{h_k}\left(z - \frac{1}{2}(z_k + z_{k+1})\right)\right]$ for displacements $u$, $v$ $(m,n = 1,2)$, and $F_\tau$, $F_s = [1 \quad z \quad z^2]$ for displacement $w(m,n = 3)$, we obtain all terms of the equations of motion by integrating through the thickness direction. For example, the terms $L_{11}$, $L_{12}$ and $L_{13}$ are:

$$\begin{aligned} L_{11} &= \sum_{k=1}^{NL} h_k \left[-C_{11}^k \partial_x^2 - 2C_{16}^k \partial_x \partial_y - C_{66}^k \partial_y^2\right] L_{12} \\ &= \sum_{k=1}^{NL} \left(\frac{z_{k+1}^2 - z_k^2}{2}\right) \left[-C_{11}^k \partial_x^2 - 2C_{16}^k \partial_x \partial_y - C_{66}^k \partial_y^2\right] L_{13} \\ &= \sum_{k=1}^{NL} (-1)^k \\ &\quad \times \frac{2}{h_k} \left( \left(\frac{z_{k+1}^2 - z_k^2}{2}\right) - \frac{1}{2} h_k (z_k + z_{k+1}) \right) \left[-C_{11}^k \partial_x^2 - 2C_{16}^k \partial_x \partial_y - C_{66}^k \partial_y^2\right] \end{aligned} \tag{34}$$

For the sake of brevity, the other terms are not presented here.

Similarly, the non-zero boundary conditions terms can be expressed by means of the fundamental nucleus $\mathbf{\Pi}^{k\tau s}$ as follows:

$$B_{ij} = \sum_{k=1}^{N_l} \int_{z_k}^{z_{k+1}} \mathbf{\Pi}_{mn}^{k\tau s} dz \tag{35}$$

## References


[1] Ferreira AJM. A formulation of the multiquadric radial basis function method for the analysis of laminated composite plates. Composite Structures 2003;59:385–92.
[2] Ferreira AJM, Roque CMC, Martins PALS. Analysis of composite plates using higher-order shear deformation theory and a finite point formulation based on the multiquadric radial basis function method. Composites: Part B 2003;34:627–36.
[3] Shu C, Ding H, Yeo KS. Local radial basis function-based differential quadrature method and its application to solve two dimensional incompressible Navier–Stokes equations. Computer Methods in Applied Mechanics and Engineering 2003;192:941–54.
[4] Wu WX, Shu C, Wang CM. Vibration analysis of arbitrarily shaped membranes using local radial basis function-based differential quadrature method. Journal of Sound and Vibration 2007;306:252–70.
[5] Bellman RE, Kashef BG, Casti J. Differential quadrature: a technique for the rapid solution of nonlinear partial differential equations. Journal of Computational Physics 1972;10:40–52.
[6] Shu C. Differential Quadrature and its Application in Engineering. Springer; 2000.
[7] Shu C, Richards BE. Application of generalized differential quadrature to solve two-dimensional incompressible Navier–Stokes equations. International Journal for Numerical Methods in Fluids 1992;15:791–8.
[8] Malekzadeh P, Karami G, Farid M. Dqem for free vibration analysis of timoshenko beams on elastic foundations. Computational Mechanics 2003;31:219–28.
[9] Malekzadeh P, Karami G, Farid M. A semi-analytical dqem for free vibration analysis of thick plates with two opposite edges simply supported. Computer Methods in Applied Mechanics and Engineering 2004;193:4781–96.
[10] Bert CW, Malik M. Differential quadrature method in computational mechanics: a review. Applied Mechanics Review 1996;49(1):1–28.
[11] Lekhnitskii SG. Strength calculation of composite beams. Vestnik inzhen i tekhnikov 1935;9.
[12] Lekhnitskii SG, Anisotropic Plates. 2nd Ed, Translated from the 2nd Russian Ed by S W Tsai and Cheron, Bordon and Breach, 1968.
[13] Ambartsumian S A, Anisotropic Plates. Fizmatzig, Moskwa; Translated from Russian, NASA TTF-118, (1964), 1961.
[14] S.A. Ambartsumian, Theory of Anisotropic Plates, in: Translated from Russian T Cheron and Edited by J E Ashton Tech Pub Co, 1969.
[15] Reddy JN. Bending of laminated anisotropic shells by a shear deformable finite element. Fibre Science and Technology 1982;17:9–24.
[16] Carrera E. Historical review of zig-zag theories for multilayered plates and shells. Applied Mechanics Reviews 2003(56):287–308.
[17] Murakami H. Laminated composite plate theory with improved in-plane response. Journal of Applied Mechanics 1986(53):661–6.
[18] Carrera E. Theories and finite elements for multilayered plates and shells: a unified compact formulation with numerical assessment and benchmarking. Archiv Comput Methods 2003;10(3).
[19] Carrera E. Developments, ideas and evaluations based upon the Reissner's mixed theorem in the modeling of multilayered plates and shells. Applied Mechanics Review 2001(54):301–29.
[20] Carrera E. On the use of Murakami's zig-zag function in the modeling of layered plates and shells. Computers & Structures 2004(82):541–54.
[21] Brischetto S, Carrera E, Demasi L. Improved bending analysis of sandwich plate by using zig-zag function. Composite Structures 2009;89:408–15.
[22] Demasi L. Refined multilayered plate elements based on Murakami zig-zag functions. Composite Structures 2005;70:308–16.
[23] Ferreira AJM, Roque CC, Carrera E, Cinefra M. Analysis of thick isotropic and cross-ply laminated plates by radial basis functions and unified formulation. Journal of Sound and Vibration 2011(330):771–87.
[24] Rodrigues JD, Roque CC, Ferreira AJM, Carrera E, Cinefra M. RBF-FD collocation and a unified formulation for bending, vibration and buckling analysis of laminated plates, according to Murakami's zig-zag theory. Composite Structures 2011(93):1613–20.
[25] Srinivas S, Rao AK. Bending, vibration and buckling of simply supported thick orthotropic rectangular plates and laminates. International Journal of Solids and Structures 1970(6):1463–81.
[26] Liew KM, Ng TY, Zhang JZ. Differential quadrature-layerwise modeling technique for three-dimensional analysis of cross-ply laminated plates of various edge-supports. Computer Methods in Applied Mechanics and Engineering 2002(191):3811–32.
[27] Zhang JZ, Ng TY, Liew KM. Three-dimensional theory of elasticity for free vibration analysis of composite laminates via layerwise differential quadrature modelling. International Journal for Numerical Methods in Engineering 2003:1819–44.
[28] Carrera E. $C^0$ Reissner–Mindlin multilayered plate elements including zig-zag and interlaminar stress continuity. International Journal of Numerical Methods in Engineering 1996;39:1797–820.
[29] Carrera E, Kroplin B. Zig-zag and interlaminar equilibria effects in large deflection and post-buckling analysis of multilayered plates. Mechanics of Composite Materials and Structures 1997;4:69–94.
[30] Carrera E. Evaluation of layer-wise mixed theories for laminated plate analysis. AIAA Journal 1998(36):830–9.

[31] Reddy JN. Energy and Variational Methods in Applied Mechanics. John Wiley; 1984.

[32] Reddy JN, Chao WC. A comparison of closed-form and finite-element solutions of thick laminated anisotropic rectangular plates. Nuclear Engineering and Design 1981;64:153–67.

[33] Pagano NJ. Exact solutions for rectangular bidirectional composites and sandwich plates. Journal of Composite Materials 1970;4:20–34.

[34] Khdeir AA, Librescu L. Analysis of symmetric cross-ply elastic plates using a higher-order theory. Part II: buckling and free vibration. Composite Structures 1988;9:259–77.

[35] Liew KM, Huang YQ, Reddy JN. Vibration analysis of symmetrically laminated plates based on fsdt using the moving least squares differential quadrature method. Computer Methods in Applied Mechanics and Engineering 2003;192:2203–22.

[36] Khdeir AA, Librescu L. Analysis of symmetric cross-ply elastic plates using a higher-order theory. Part II: buckling and free vibration. Composite Structures 1988;9:259–77.

[37] Liew KM, Huang YQ. Bending and buckling of thick symmetric rectangular laminates using the moving least-squares differential quadrature method. International Journal of Mechanical Sciences 2003;45:95–114.

[38] Liew KM, Chen XL, Reddy JN. Mesh-free radial basis function method for buckling analysis of non-uniformly loaded arbitrarily shaped shear deformable plates. Computer Methods in Applied Mechanics and Engineering 2004;193:205–24.

[39] Liew KM, Chen XL. Mesh-free radial point interpolation method for the buckling analysis of Mindlin plates subjected to in-plane point loads. International Journal of Numerical Methods in Engineering 2004;60:1861–77.

[40] Liew KM, Chen XL. Buckling of rectangular Mindlin plates subjected to partial in-plane edge loads using the radial point interpolation method. International Journal of Solids and Structures 2004;41:1677–95.